2011 IEEE Conference on Sustainable Utilization and Development in Engineering and Technology (STUDENT)
The University of Nottingham, Semenyih, Selangor, Malaysia. 20-21 October 2011.

Control of a Cable-Driven 2-DOF Joint Module with a Flexible Backbone

Tran L.D., Zhang Z., Yeo S.H.
School of Mechanical and Aerospace Engineering
Nanyang Technological University, Singapore
Email: tran0055@e.ntu.edu.sg; M080005@e.ntu.edu.sg;
MYEOSH@ntu.edu.sg;

Sun Y.C., Yang G.L.
Singapore Institute of Manufacturing and Technology
Email: glyang@simtech.a-star.edu.sg;
ycsun@simtech.a-star.edu.sg;

Abstract—**Dexterous robotic arms have gained increasing attention in the robotics community in recent years, especially snake-like robots. A cable-driven snake-like robot arm (CDSLRA) owns a number of promising advantages such as: light-weight structure, low energy consumption, high speed motion due to low moment inertia and it is suitable to work in constrained work-conditions. A prototype consisting a series of 2-degree of freedom (DOF) joint modules with flexible backbone is proposed in this research. The kinematic analysis of n-module CDSLRA with flexible backbone is performed and developed. In addition, the design and implementation of motion control is also discussed. Set of PID parameters from analytical approach and experiments are obtained and compared for step response of the servo motor. From the experiments, the 2-DOF joint module with flexible backbone shows good position control and tracking ability.**

Keywords – Snake-like robot arm; Cable-driven; Motion Control; Flexible backbone.

I. INTRODUCTION

In recent years, there are increasing interest among the researchers on the design and analysis of hybrid parallel and serial mechanisms. Parallel mechanisms can achieve high velocity as well as high acceleration that in serial manner is impossible [1], while serial mechanism provides large work-space. Dexterous robotic arms with combination of 2 mecha-nisms have gained attentions in the robotics community recently due to their high flexibility [2][3][4]. A snake-like robot is typical example of dexterous robotic arms with redundant degree of freedom. It can move on narrow place and a place with a height difference. There are two different kinds of snake-like robots: discrete and continuous robots. The key advantage of using discrete robots is that the motion of the snake robot is predictable. However, its disadvantage is that they cannot provide high output speed. In contrast, due to their capability of bending continuously, continuum robots can achieve higher speeds relative to their discrete counterparts but the motion is unpredictable. Our target is design a robot that combines advantages of both: high output speed and predictable motion.

Currently, most of robot manipulators' mechanisms are conventional mechanisms that consist of a number of rigid links and joints. Using cable instead of linkages gives us simple mechanical and light-weight structure, low energy consumption [5]; large workspace, limited by cable lengths and cable tension constraints; low moment inertia and high speed motion; easy reconfigurability. So far, there are a lot of researches conducted in workspace analysis and optimal design of cable-driven planar parallel manipulators [6], stiffness analysis [7], dynamic and control [8][9], tension analysis in CDPM [10]. But, the kinematic analysis of cable length required more efforts and the cable has always to be in the tensile state to avoid the sagging. In general, CDPM is classified by 3 categories [11], based on the number of cables (m) and number of DOF (n): incompletely restrained ($m < n+1$), fully restrained ($m = n+1$), redundantly restrained ($m > n+1$). In completely restrained and redundantly restrained systems, the pose can be completely determined by the function of cable lengths. The applications with high speed, high acceleration or high stiffness prefer using these configurations. Increasing redundancy of CDPM will improve the stability of the system, however it requires more motors as well as reduces number of DOF due to extra constrains [9]. Those applications requiring high speed operation, accuracy; dealing in constrained workspace or replacing human appearance can be satisfied by using CDSLRA, such as: repairing and maintenance in Nuclear industry; Manufacture and assembly inside wing boxes, jet engines; search and rescue. In this research, the CDSLRA is a serial mechanism formed by linking individual parallel mechanism modules with fully restrained configuration together.

Previous research on CDSLRA has been with universal joint prototype [14]. It has been implemented well with position control by formulating kinematic model. In current research, the proposal prototype with flexible backbone gives some advantages over universal joint prototype. By using flexible backbone, it provides lower cost of fabrication; reducing robotic arm's weight; increasing flexibility, velocity in motion. Kinematic analysis including inverse and forward formulation is established fully for n-module CDSLRA with flexible backbone. Moreover, motion control and trajectory planning with experiment are also conducted to clarify the correctness of kinematic formulation.

II. KINEMATIC ANALYSIS OF N-MODULE CDSLRA WITH FLEXIBLE BACKBONE

A. Module Design:

The proposed design of CDSLRA adopts a modular approach, consisting a number of serially connected joint modules. Fig. 1 shows the design of the standard joint module. The module comprising a base disk, a moving platform and 3 cables is conducted in research consists a series of modules. The cables are located equally at 120^0 apart. The backbone is made of elastic and inextensible materials, and is rigid in torsion. Hence, the joint module can be considered as having 2-DOF. For current prototype, stainless steel cables and Delrin backbone are employed.

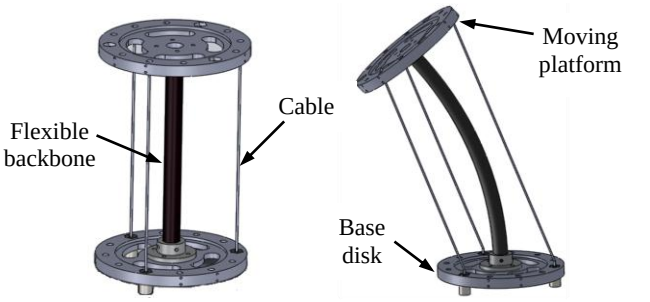

Figure 1. Two-DOF Joint Module design

The orientation of each module in 3-D can be described by the Euler angle parameters [13] as shown in Fig.2. In Euler angle representation, any orientation can be modeled by 3 angles: the rotating angle (ϕ), the tilt angle (θ) and the roll angle (ψ).

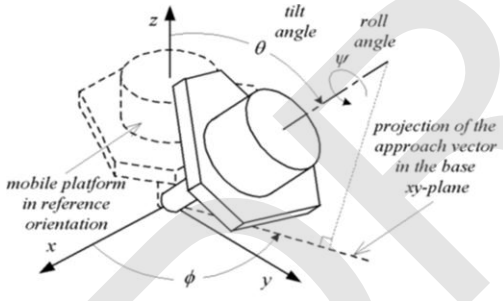

Figure 2. Set of Euler angles for platform's orientation [13]

For the proposed joint module, there is no torsional rotation i.e. ψ=0. The rotational matrix can be expressed by:

$$\mathbf{R}(\phi,\theta) = \mathbf{R_z}(\phi)\mathbf{R_y}(\theta)\mathbf{R_z}(-\phi) = \begin{bmatrix} c_\phi{}^2 c_\theta + s_\phi{}^2 & s_\phi c_\phi c_\theta & c_\phi s_\theta \\ s_\phi c_\phi c_\theta & s_\phi{}^2 c_\theta + c_\phi{}^2 & s_\phi s_\theta \\ -c_\phi s_\theta & -s_\phi s_\theta & c_\theta \end{bmatrix} \quad (1)$$

in which: $s_\phi = \sin\phi$, $c_\phi = \cos\phi$, $s_\theta = \sin\theta$, $c_\theta = \cos\theta$

B. Kinematic Analysis:

Fig. 3 shows the block diagram of the kinematic analysis for joint module (j). The forward kinematics is presented under sub-sections 1a & 2b and the inverse kinematics is covered in sub-sections 1b & 2a for n-module robotic arm. Global frame {G} is attached at the fixed platform of the first module. Each set of angles comprises 2 components that reflect relative orientation of base disk with the moving platform for each module. Note that the moving platform of one module is considered as the base disk of the next module.

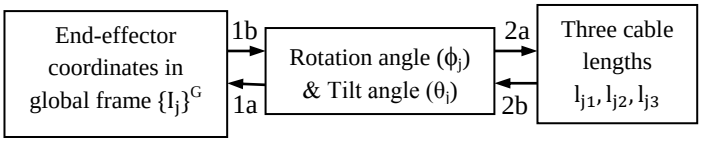

Figure 3. Kinematic analysis block diagram

1) Relationship between End-effector Coordinate in Global frame and Orientation Angles

Three coordinate systems are defined for $(j)^{th}$ module as shown in Fig.4. The end-effector is denoted as I_j

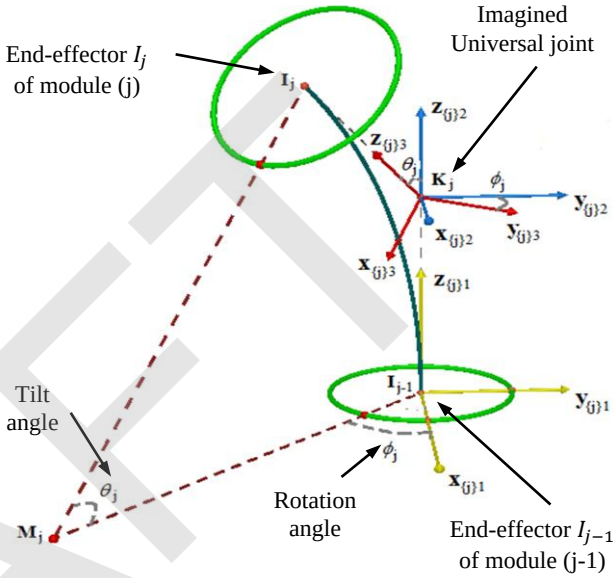

Figure 4. Coordinate system for $(j)^{th}$ module

a) From Orientation angles to find End-effector Coordinate in {G}: $\{I_j\}^G$ of each Module

For any displacement of the end-effector, the bending shape of the backbone is assumed to be circular with a constant arc length L_0. If the tilt angle of the module is θ_j, then the radius of the arc is $R_j = L_0/\theta_j$. Since the gradients at the 2 end-points of the arc are geometrically perpendicular to the respective platforms, the flexible backbone configuration can be considered as a universal joint with its center at K_j and arm length defined by:

$$L_j = |\overrightarrow{K_j I_j}| = |\overrightarrow{K_j I_{j-1}}| = \left(\frac{L_0}{\theta_j}\right)\tan\left(\frac{\theta_j}{2}\right) \quad (2)$$

Based on universal joint configuration, 3 frames defined are related as follows:

$$\text{Frame } \{j\}_1 \xrightarrow[(0\ 0\ L_j)]{\text{Translating}} \text{Frame } \{j\}_2 \xrightarrow[R(\phi_j,\theta_j)]{\text{Rotating}} \text{Frame } \{j\}_3$$

Global frame {G} corresponds to frame $\{1\}_1$ of module 1 attached with base plate. The transformation matrix from frame $\{j\}_3$ to frame {G} is:

$$\begin{matrix}\{G\}\\\{j\}_3\end{matrix}\mathbf{T} = \begin{matrix}\{1\}_1\\\{1\}_2\end{matrix}\mathbf{Q}\begin{matrix}\{1\}_2\\\{1\}_3\end{matrix}\mathbf{R}\{\prod_{k=2}^{k=j}\left(\begin{matrix}\{k-1\}_3\\\{k\}_2\end{matrix}\mathbf{Q}\begin{matrix}\{k\}_2\\\{k\}_3\end{matrix}\mathbf{R}\right)\} \quad (3)$$

by which:

$\begin{matrix}\{1\}_2\\\{1\}_3\end{matrix}\mathbf{R}$; $\begin{matrix}\{k\}_2\\\{k\}_3\end{matrix}\mathbf{R}$ reflect rotation matrix of module 1; module k respectively, obtained by substituting set of orientating angles (ϕ_1, θ_1); (ϕ_k, θ_k) into (1).

$${}^{\{1\}_2}_{\{1\}_3}\mathbf{R} = \begin{bmatrix}\mathbf{R}(\phi_1,\theta_1) & 0\\ 0 & 1\end{bmatrix}; {}^{\{k\}_2}_{\{k\}_3}\mathbf{R} = \begin{bmatrix}\mathbf{R}(\phi_k,\theta_k) & 0\\ 0 & 1\end{bmatrix}$$

${}^{\{k-1\}_3}_{\{k\}_2}\mathbf{Q}$; ${}^{\{1\}_1}_{\{1\}_2}\mathbf{Q}$ refer to translating matrix between frames, their values are represented by following matrix:

$${}^{\{j-2\}_3}_{\{j-1\}_2}\mathbf{Q} = \begin{bmatrix}\mathbf{I}_{3x3} & \begin{pmatrix}0\\0\\L_{j-1}+L_{j-2}\end{pmatrix}\\ 0 & 1\end{bmatrix}; {}^{\{1\}_1}_{\{1\}_2}\mathbf{Q} = \begin{bmatrix}\mathbf{I}_{3x3} & \begin{pmatrix}0\\0\\L_1\end{pmatrix}\\ 0 & 1\end{bmatrix}$$

With corresponding tilt angles of each module and (2), we can get those values $L_{j-1}; L_{j-2}; L_1$.

The coordinate of end-effector I_j of j^{th} module is defined as $\{I_j\}^{\{j\}_3} = (0 \;\; 0 \;\; L_j)$ in frame $\{j\}_3$. Likewise, its coordinates in global frame is given by $\{I_j\}^G$ and expressed in following formula:

$$\begin{bmatrix}\{I_j\}^G\\ 1\end{bmatrix}_{4\times1} = {}^{\{1\}_1}_{\{j\}_3}\mathbf{T}\begin{bmatrix}\{I_j\}^{\{j\}_3}\\ 1\end{bmatrix}_{4\times1} \quad (4)$$

the target of finding $\{I_j\}^G$ can be achieved by evaluating ${}^{\{1\}_1}_{\{j\}_3}\mathbf{T}$ from (3).

b) Determining Angle Orientation for each Module based on end-effector coordinate in global frame:

Here, the purpose is to find the tilt angle (θ) and rotating angle (ϕ) of each module with assumption: end-effector coordinates I_j of all modules in global frame $(X_{I_j}, Y_{I_j}, Z_{I_j})$ are given.

Considering module 1 and its end-effector, the transformation matrix from frame $\{1\}_3$ to global frame is

$$\begin{pmatrix}X_{I_1}\\ Y_{I_1}\\ Z_{I_1}\end{pmatrix} = \begin{pmatrix}L_1\cos\phi_1\sin\theta_1\\ L_1\sin\phi_1\sin\theta_1\\ L_1\cos\phi_1 + L_1\end{pmatrix}$$

Equating both sides

$$\therefore \phi_1 = \tan^{-1}\left(\frac{Y_{I_1}}{Z_{I_1}}\right); \theta_1 = \cos^{-1}\left(\frac{-A+1}{A+1}\right) \text{ with } A = \left(\frac{Y_{I_1}}{Z_{I_1}}\sin\phi_1\right)^2$$

Therefore arm magnitude of imagined universal joint is:

$$\text{From equation (2)} \rightarrow L_1 = \left(\frac{L_0}{\theta_1}\right)\tan\left(\frac{\theta_1}{2}\right)$$

Using inductive method in mathematics, assuming all the sets: (ϕ_k, θ_k, L_k) with $k = 1..(j-1)$ are determined, we will find those values (ϕ_j, θ_j, L_j)

Using ${}^{\{1\}_1}_{\{j\}_3}\mathbf{T}$ from (3); coordinate of end-effector I_j of j^{th} module in frame $\{j\}_3$: $\{I_j\}^{\{j\}_3} = (0 \;\; 0 \;\; L_j)$, coordinate of end-effector I_j in global frame{G}: $\{I_j\}^G = (X_{I_j} \;\; Y_{I_j} \;\; Z_{I_j})$ and equation (4)

$$\therefore \begin{bmatrix}X_{I_j}\\ Y_{I_j}\\ Z_{I_j}\\ 1\end{bmatrix} = \begin{bmatrix}\mathbf{R}_{(\phi_1,\theta_1)} & \begin{pmatrix}0\\0\\L_1\end{pmatrix}\\ 0 & 1\end{bmatrix}\prod_{j=2}^{k=j}\begin{bmatrix}\mathbf{R}_{(\phi_k,\theta_k)} & \begin{pmatrix}0\\0\\L_{k-1}+L_k\end{pmatrix}\\ 0 & 1\end{bmatrix}\begin{bmatrix}0\\0\\L_j\\1\end{bmatrix}$$

Multiplying both sides with inverse matrix of those in right hand side, we get set of orientation angles of module (j)

$$\rightarrow \phi_j = \tan^{-1}\left(\frac{b_j}{a_j}\right); \theta_j = \cos^{-1}\left\{\frac{-B+1}{B+1}\right\} \text{ with } B = \left(\frac{b_j}{j}\sin\phi_j\right)^2$$

in which a_j, b_j, c_j are obtained from calculation

$$\begin{bmatrix}a_j\\ b_j\\ c_j\\ 1\end{bmatrix} = \prod_{k=j-1}^{k=2}\begin{bmatrix}\mathbf{R}_{(\phi_k,\theta_k)} & \begin{pmatrix}0\\0\\L_{k-1}+L_k\end{pmatrix}\\ 0 & 1\end{bmatrix}^{-1}.$$

$$\begin{bmatrix}\mathbf{R}_{(\phi_1,\theta_1)} & \begin{pmatrix}0\\0\\L_1\end{pmatrix}\\ 0 & 1\end{bmatrix}^{-1}\begin{bmatrix}X_{I_j}\\ Y_{I_j}\\ Z_{I_j}\\ 1\end{bmatrix} - \begin{bmatrix}0\\0\\L_{j-1}\\1\end{bmatrix}$$

$\mathbf{R}_{(\phi_k,\theta_k)}, \mathbf{R}_{(\phi_1,\theta_1)}$ are rotation matrix for module k and 1 respectively

$L_{k-1}; L_{k-2}; L_1; L_{j-1}$ are from equation 2 with substitution of corresponding tilting angles for each module

2) Relationship between Cable length and Orientation Angles

a) Given Rotation and Tilt angles, finding Cable Lengths for each Module

It is necessary to evaluate the cable lengths based on a set of orientated angles. Fig. 5 shows the configuration of j^{th}-module with 3 cables. Points B_{ji} and P_{ji} (i=1,2,3) are the end-points of i^{th} cable linking the base disk and the moving platform. The length of vector $\overrightarrow{B_{j1}P_{j1}}$, (i=1,2,3) represents the cable length l_{ji} of i^{th} cable.

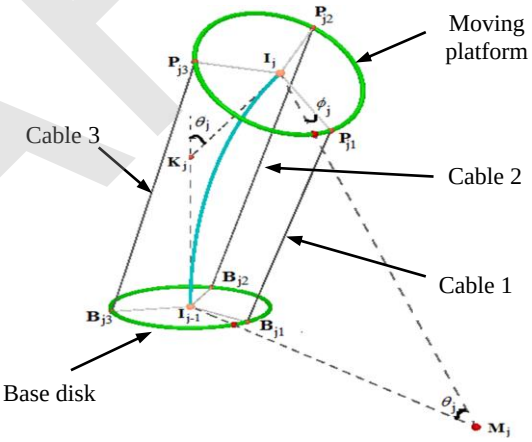

Figure 5. Configuration of $(j)^{th}$ module

A loop-closure equation for i^{th} cable can be written as:

$$\overrightarrow{P_{j1}B_{j1}} = \overrightarrow{P_{j1}I_j} + \overrightarrow{I_jK_j} + \overrightarrow{K_jI_{j-1}} + \overrightarrow{I_{j-1}B_{j1}}$$

All the vectors are represented in frame $\{j\}_1$ i.e. with respect to the base platform of j^{th} module , therefore:

$$\overrightarrow{P_{j1}B_{j1}} = \left(\mathbf{I}_{3x3} - \mathbf{R}_{(\phi_j,\theta_j)}\right)\begin{pmatrix}r\cos(j\pi - 2\pi(i-1)/3)\\ r\sin(j\pi - 2\pi(i-1)/3)\\ 0\end{pmatrix} + \begin{pmatrix}0\\0\\L_j\end{pmatrix} \quad (5)$$

r is platform's radius, L_j is imaged universal joint's arm of j^{th} module. Hence, cable length is determined by taking magnitude of $\overrightarrow{P_{j1}B_{j1}}$

b) Finding Orientation Angles based on Cable's Lengths

Geometrically, the three cables within a joint module are parallel:

$$P_{j1}B_{j1} // P_{j2}B_{j2} // P_{j3}B_{j3} // I_{j-1}I_j$$

Then titling angle θ_j can be obtained from following equation, in which L_0 is backbone length:

$$\sin\left(\frac{\theta_j}{2}\right) = \frac{\theta_j(l_{j1} + l_{j2} + l_{j3})}{12L_0}$$

Cable 1 in module (j) is connection connected 2 points: B_{j1} and P_{j1}. To differentiate cable 1 with other cables in same module, the location of point B_{j1} should be determined. Location of point B_{j1} is located in base disk of module (j). If j is odd number, location of point B_{j1} is at point 2; otherwise it is at point 1(as shown in Fig.6).

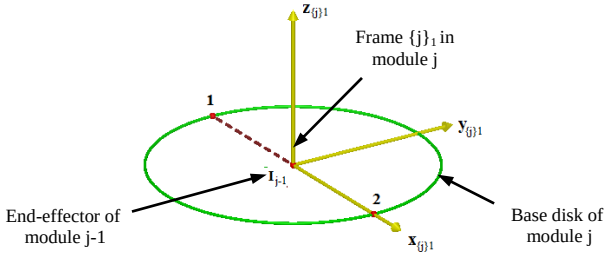

Figure 6. Position of point B_{j1} in $(j)^{th}$ module

The relationship between cable1's length and set of orientation angles in j^{th} module is obtained from equation (5):

$$l_{j1}{}^2 = \left[(-1)^{j+1} r\left(1 - c_\phi{}^2 c_\theta - s_\phi{}^2\right) + L_j c_\phi s_\theta\right]^2 + \left[(-1)^{j+1} r\left(s_\phi c_\theta c_\phi - s_\phi c_\phi\right) + L_j s_\phi s_\theta\right]^2 + \left[(-1)^j r s_\theta c_\phi + L_j(1 + c_\theta)\right]^2$$

where $s_\phi = \sin\phi$, $c_\phi = \cos\phi_j$, $s_\theta = \sin\theta_j$, $c_\theta = \cos\theta_j$, r is platform's radius, L_j is imaged universal joint's arm of j^{th} module

By rearranging the terms, a quadratic equation is obtained :

$$Ac_\phi{}^2 + Bc_\phi + C = 0$$

$$A = 2r^2(c_\theta - 1), B = (-1)^{j+1} \times 4L_j r s_\theta,$$

and $C = l_{j1}{}^2 - 2L_j{}^2(1 + c_\theta)$

$$\therefore \phi_j = \cos^{-1}\left(\frac{-B \pm \sqrt{B^2 - 4AC}}{2A}\right)$$

III. Motion Control

A two-module CDSLRA prototype with flexible backbone is shown in Fig.7:

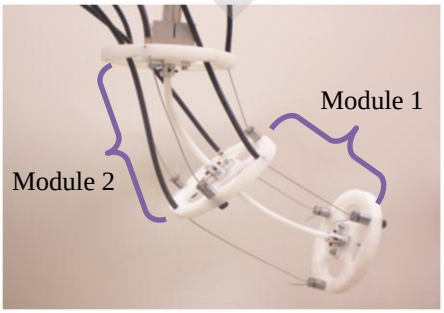

Figure 7. Cable-driven dexterous robotic arm prototype

A. Position Control System

To control the movement of one module with 2 DOF, there are necessarily 3 cables attached between 2 platforms. The position controlled motion system operates based on the incremental encoder feedback, shown in Fig.8. Proportional–integral–derivative (PID) Controller drives the motion of Brushless DC servomotors (EC45-136198). Initially, trajectory constraints including: position, velocity, acceleration and jerk are set in Measurement & Automation Explorer (MAX), a graphical user interface provided by National Instruments (NI). The NI motion controller PCI-7350 received command from Labview software as well as MAX. After that, "Trajectory Generation" is created for motor to get target position. PID controller will manipulate the position error between the desired position and actual position to maintain the required motion. The B15A8 amplifier receives signal from PID controller in Voltage using Digital-to-Analog Convertor (DAC) and provides corresponding current to run motor. An incremental encoder is attached in shaft of motor to record the current position of motor and to send the feedback into controller for adjusting commanded signal and providing desired position.

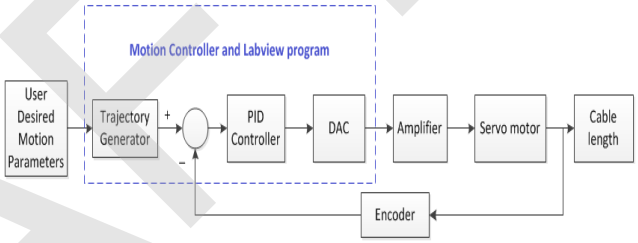

Figure 8. Position Control Loop

B. Software Development

1) PID Tuning:

Set of PID parameters is investigated by both experimental analytical methods to make smooth and fast response from motor.

a) Experimental Approach:

Conducting step response in Servo Tune of MAX, with step length as 1000 counts and samples as 200; set of values K_P, K_D, K_I is found for current device setup, with settling time = 123ms.

b) Analytical Approach:

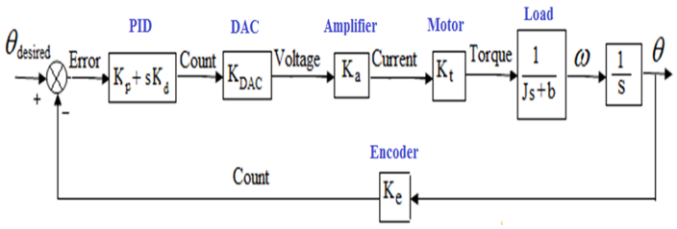

Figure 9. Mathematical model of transfer function

All devices are modelled as constant parameters shown in Fig. 9; in which, K_P and K_D: proportional and derivative gains of PID in z domain; K_{DAC}, K_a: the gains of digital-to-analogue convertor and amplifier; K_t: torque constant of motor; J is rotor inertia, viscous damping b≈0 for current setup and can be neglected; K_e the transfer function of encoder. The target is

to find set of PID parameters corresponding with set of settling times and overshoots: t_s =0.05s, %M= 10 (due to viscous friction of system, it will help to cancel overshoot). Using overshoot and settling time formula:

$$\%M = \exp(-\pi*\zeta/\sqrt{1-\zeta\hat{}2}),\ t_s = 4.6/(\zeta*\omega_n)$$

find ω_n, ζ and corresponding closed-loop poles in s domain for set of response requirements.

Continuous approximation approach

All the models of the mixed s-domain and z-domain system are all converted to the s-domain. When the sampling time T is small, the effect of the zero order hold is neglected.

The open-loop transfer function of system:

$$L_{(s)} = (K_P + K_D s) * K_{DAC} * K_a * K_t * 1/(Js) * 1/s * K_e \quad (6)$$

in which $K_P = k_p$; $K_D = k_D/T$; $K_I = T*k_I$ (T:sampling time).

PID constants are found by using conditions:$|L(j\omega_c)| = 1$ and $\angle L(j\omega_c) = y - \pi$ with formula:

$$\omega_c \approx \omega_n\sqrt{(1-2\zeta^2) + \sqrt{4\zeta^4 - 4\zeta^2 + 2}}$$

$$\gamma = \tan^{-1}\left(2\zeta/\sqrt{-2\zeta^2 + \sqrt{1+4\zeta^4}}\right)$$

Digital approach

After a controller is designed using the continuous approximation method, it is important to perform a z-domain analysis since the final control scheme is eventually implemented on a microprocessor and it is desirable to see the effect of the designed D(s) controlling the system. We look at the poles and zeros on the z-plane in the same manner as we look for them in the s-plane. The main difference is that for stability, the closed loop poles must be inside the unit circle on the z-plane.

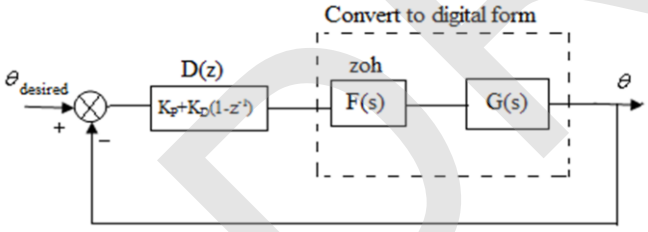

Figure 10. Control loop representation for position control

The zoh has a transfer function of the form:

$$F(s) = (1 - e^{-Ts})/s$$

With G(s) is the open loop of system without PID controller and equal to L(s) in equation (6), the transformation into z-domain of $F(s)G(s)$ is:

$$G_0(z) = Z\{F(s)G(s)\}$$

The closed-loop transfer function of the system:

$$T(z) = D(z)G_0(z)/(1 + D(z)G_0(z)) \quad (7)$$

Using the pole-zero mapping: $z = e^{sT}$ and closed-loop poles in s-domain to find corresponding closed-loop poles in z-domain. Find suitable K_D and K_p parameters by substituting closed-loop poles into characteristic equation of T(z). After finding K_D and K_p, $K_I = 1$ is added to the PD controller to eliminate the steady-state error. The analytical approach with set 1 requirement from table 1 gives better response (settling time is only 83ms comparing to 123ms of experimental approach).

2) Labview programming:

Purpose of Labview program is to control motor's operation and make sure all motors pull or release cables simutaneously in one robotic arm's movement. Assuming two motors accelerate and decelerate in the same duration t_1, motor 1 will achieve velocity V_1 after accelerating with A_1, while motor 2 achieves V_2.after accelerating with A_2. Labview will activate motor operating to satisfy condistions:

$\frac{A_1}{A_2} = \frac{V_1}{V_2} = \frac{\Delta L_1}{\Delta L_2}$ in which $\Delta L_1, \Delta L_2$ represent the change in cable length for cables connected with each motor.

IV. Result and Discussion

A. Position Control Experiment:

For accuracy of position control, the experiment in this project is conducted in one module prototype with 12 sets of tilt (θ) and rotation (ϕ) angles (tilt angles are set from: 30^0-60^0), the experimental and analytical values of 3 cables as well as distance between endpoint and global coordinate's origin (known as end-effector distance, as described in Fig.9) are evaluated .

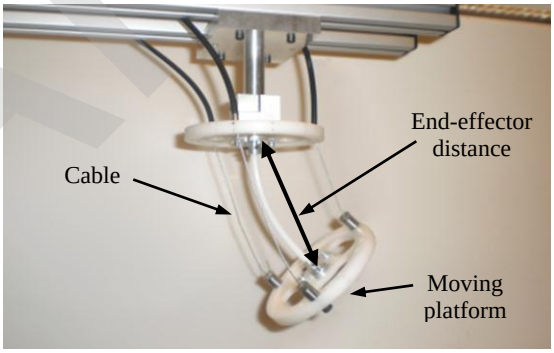

Figure 11. Feature of robotic arm with one module

The percentage errors between the experimental and analytical values are shown in Fig.12.

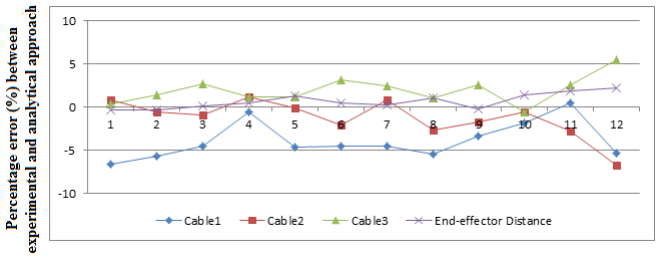

Figure 12. Percentage error for position control experiment

For the end-effector distance, the difference between the experimental and analytical values is smaller than 2.5%. This shows that the assumptions made in the kinematic analysis are valid i.e. the length of backbone remains the same during the bending and the equivalent universal joint module configuration. For the cable length, the results from the experimental approach are close to the values obtained from kinematic analysis with an average error of about 3%.

B. Trajectory Planning Experiment:

Basically, tracking path of robotic arm can be divided into small sections classified with 2 kinds of segment: straight and arc. In this experimental study, we conduct the trajectory planning for 1 module model with circular path. A pen is attached at end of robotic arm and constructing circular path when desired trajectory path is set in Labview. Fig.13 shows the Matlab drawing for trajectory planning experiment. The circle radius for tracking path of end-effector is commanded into Labview program. Program will activate motors and make robotic arm track along a circular path. A pen is attached at end-effector point, therefore pen's tracking path can be recorded into blank paper.

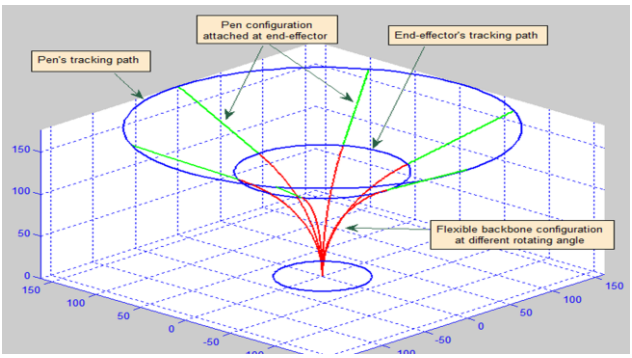

Figure 13. Visualization of path for trajectory planning

To evaluate tracking ability of robotic arm, radius of pen's tracking path is recorded and compared with analytical value obtained Matlab program. Range of tilting angles of module are tested from 20^0 to 60^0. Results are shown in Fig.14. We can obviously realize that experimental results almost follow analytical results:

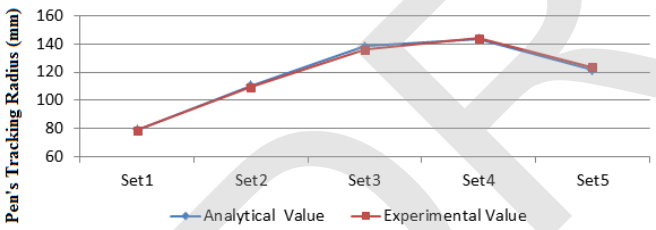

Figure 14. Circle radius of tracking path for trajectory planning

By observing and evaluating results, current robotic arm prototype has good tracking ability with tiling angles from 20^0 to 60^0. The more steps we divide circular path, the nicer and more accurate path we can obtain.

V. Conclusion and Future Work

In this paper, the kinematic formulation for CDSLRA with flexible backbone is presented. Comparing with previous rigid joint design, the proposed prototype with flexible backbone has lower cost of fabrication, and with reduced weight and increased flexibility. It has been shown that the kinematic formulation of the flexible backbone joint module can be modeled as an equivalent universal joint having arm length varying with the tilt angle. The kinematic formulation is applicable for n-module robotic arm. The PID parameters from analytical approach and experiments are obtained and compared for step response of the servo motor. The values are used in the position control as well as trajectory planning for the 2-DOF joint module with flexible backbone. From the experiments, it is seen that good position control and tracking ability are achieved. The percentage error in position control is found to be less than 3%. For application, the prototype in current research can work well in many fields that require high speed operation, accuracy; deal in constrained workspace and some replaces the appearance of human.

For future work, the motion control and trajectory planning will be extended to the arm level with many joint modules. In addition, it will be challenging to implement both position and tension control on cable-driven mechanism to ensure that the desired position can be reached while keeping all the cables in tension during movement.

Acknowledgment

We wish to acknowledge the funding support for this project from Nanyang Technological University and SIMTech under the Undergraduate Research Experience on Campus (URECA) programme.

References

[1] P. Gholami, M. Aref, and H.Taghurad, "On the Control of the KNTU CDRPM: A Cable Driven Redundant Parallel Manipulator", *IEEE/RSJ International Conference on Intelligent Robots and Systems*, pp. 2404-2409, Nice, France, 2008.

[2] I.A. Gravagne, "Asymptotic regulation of a one-section continuum manipulator", *IEEE/RSJ International Conference on Intelligent Robots and Systems*, vol. 3, pp. 2779-2784, Las Vegas, USA, 2003.

[3] M. Yamakita, M. Hashimoto, and T. Yamada, "Control of locomotion and head configuration of 3D snake robot (SMA)", *IEEE International Conference of Robotics and Automation*, vol. 2, pp. 2055-2060, Taipei, Taiwan, 2003.

[4] F. Matsuno, and K. Suenaga, "Control of redundant snake robot based on kinematic model", *41th SICE Annual Conference*, vol. 3, pp. 1481-1486, Osaka, Japan, 2002.

[5] R.L. Williams, P. Gallina, and J. Vadia, "Planar Translational Cable-Direct Driven Robots", *Journal of Robotic Systems*, vol. 20, no 3, pp. 107-120, 2003.

[6] C.B. Pham, S.H. Yeo, and G.L. Yang, "Workspace analysis and optimal design of cable-driven planar parallel manipulators", *IEEE Conference on Robotics, Automation and Mechatronics*, pp. 219–224, Singapore, 2004.

[7] S. Sahin, and L. Notash, "Kinematics, workspace and stiffness analysis of wire-actuated parallel manipulators", *World Congress in Mechanism and Machine Science*, pp. 1868–1872, Tianjin, China, 2004.

[8] A.B. Alp, and S.K. Agrawal, "Cable suspended robots: Design, planning and control", *IEEE Conference on Robotics and Automation*, pp. 4275–4280, Washington, DC, USA, 2002.

[9] R.L. Williams, and P. Gallina, "Planar cable-direct-driven robots, part ii: Dynamics and control", *ASME Design Technical Conferences*, Pittsburgh, PA, USA, 2001.

[10] C.B. Pham, S.H. Yeo, and G.L. Yang, "Tension analysis of cable-driven parallel mechanisms", *IEEE Conference on Intelligent Robots and Systems*, pp. 257-262, Singapore, 2005.

[11] A. Ming, and T. Higuchi, "Study on multiple degree-of-freedom positioning mechanism using wires (part 2) – development of a planar completely restrained positioning mechanism", *International Journal of Japan Social Engineering*, vol. 28(3), pp. 235–242, 1994.

[12] Y. Yi, J.E. Mclnroy, and Y Chen, "Over-constrained Rigid Multi Body Systems: Differential Kinematics, and Fault Tolerance," *Smart Structures and Materials 2002: Smart Structures and Integrated Systems*, vol. 4701, pp. 189-199, 2002.

[13] I.A. Bonev, and J. Ryu, "Orientation workspace analysis of 6-dof parallel manipulators", *ASME Design Engineering Technical Conferences*, pp. 1-8, Las Vegas, USA, 1999.

[14] G.Z. Lum, S.K. Mustafa, H.R. Lim, W.B. Lim, G.L. Yang, and S.H. Yeo,"Design and motion control of a cable-driven dexterous robotic arm", *Sustainable Utilization and Development in Engineering and Technology (STUDENT), 2010 IEEE Conference*, pp. 106, Malaysia, 2010.